BURIED OBJECT LOCATION BASED ON FREQUENCY DOMAIN MEASURMENTS

K. A. Shaaban*, W. M. Hussein*, M. Soliman*, H. M. Mahgoub*

ABSTRACT

In this paper, wideband ground penetrating radar (GPR) system and a proposed frequency domain data analysis technique are presented for the detection of shallow buried objects such as anti-personal (AP) land mines. The GPR system uses one antenna for transmitting and for receiving and. it operates from 9 GHz to11 GHz. This system is able to acquire, save and analyze the data in the frequency domain. Common Offset technique has been used for acquiring and processing the data. This technique is effective for the rejection of the ground surface clutter. By applying the C-scan scheme, metallic and plastic mines-like targets buried in dry soil will be located.

KEY WORDS

Remote Sensing, GPR data analysis and Mine Detection.

----

* Egyptian Armed Forces.

INTRODUCTION

Anti-personal (AP) land mines are explosive devices placed on or beneath the surface of the Earth for destroying vehicles and killing or maiming human beings. Mines are usually deployed during a military conflict. However, they may remain in the ground undetected for decades after the cessation of hostilities. The United Nations estimates that there are currently over 100 million land mines buried in 62 countries throughout the world, and that the number of deployed mines increases by approximately 2 million each year, and accidental detonation of mines kills or maims 600 or more people a month, predominantly civilians [1]. The resulting injuries have devastating effects on the lives of the wounded and place incredible demands on the quality of life.

Since World War II, the United States army has investigated many different technologies for detecting land mines. These include the use of electromagnetic radiation over a wide spectrum: very low frequencies (metal detectors), radio and microwave frequencies, infrared and optical frequencies. The sensors operating at radio and microwave frequencies are often in the form of Ground Penetrating Radar (GPR) [2, 3, 4]. Systems for finding non-metallic land mines were also developed. Even though systems were developed and tested in the late 1960's and early 1970's for these tasks, shallow target detection remains to be one for continuing development in GPR. This application has significant difficulties due to the propagation losses in the soil, the low contrast between target and soil electrical properties in some cases, and because of large variety of clutter echoes from the rough surface and other shallow contrasts such as rocks, tree roots, etc [5].

Recently, a GPR system was reported by Sato et al. [6, 7] for detecting the shallow buried object. The system operates in the frequency range between 2 MHz and 6 GHz, and an array of broadband Vivaldi antennas was used for transmitting and receiving. The Common Mid Point (CMP) technique was applied to acquire and analyze the data. The measurements were made in frequency domain and the acquired data were converted to time domain. A migration algorithm was applied, and they demonstrated that the algorithm is effective to remove the ground surface clutter effect and that the system could detect a model of plastic land mine of 78 mm in diameter and 40 mm in height with an antenna height of 5 cm and object depth of 2 cm.

An alternative technique was proposed by Brunzell [8] for solving the problem of the ground surface clutter using the Maximum Likelihood approach. A GPR system was also demonstrated by Groenenboom et al. [9] for the landmine detection using a dielectric filled TEM horn transmitting antenna and a small loop receiver antenna below the transmitting antenna. The system operates in the frequency range 500 MHz to 2 GHz. Two-dimensional moving average subtraction was used to filter out the response of the strong surface reflection.

A stepped-frequency continuous-wave GPR, called SAR-GPR, was developed by Sato et al. [10, 11]. This system can acquire CMP data. CMP stacking and Kirchhoff migration algorithms were used to locate the landmines. UWB array-based time-

domain radar operating from 500 MHz to 3 GHz for landmine detection was also reported [12].

The review shows that the design of UWB antennas and the technique for removing the ground surface effect are two key aspects in determining the performance of a GPR system.

In this paper, we report a frequency domain GPR system that uses one antenna for transmitting and receiving operating in the frequency range between 9 GHz and 11 GHz and a frequency domain object location technique with equations presented in Section 2. The GPR system is able to acquire, save and analyse the data measured in frequency domain. Common Offset technique is used to acquire data and also for data processing, which is simple and effective for the rejection of the ground surface clutter. The system has been tested in the laboratory. Its ability to detect metallic and plastic objects by using A, B and C-scan schemes will be demonstrated using several examples in this paper. The system, principle of buried object detection and the results of experimental evaluation will be presented in the following sections.

SYSTEM SETUP

The frequency domain GPR system mentioned above is illustrated in Fig.1. The system consists of a transmitting / receiving antenna, a vector network analyzer (VNA) for the frequency domain measurement, a computer for measurement control, data analysis and result display. The operation of the system is managed by computer program, which performs two main tasks. Firstly, it acquires the transmission data in the frequency domain from 9 GHz to 11 GHz containing the information of the reflected microwave signal from the ground and/or buried objects. Secondly, it saves the data of the received signal in the form of S11-parameter at selected frequency points over the range.

Data Analysis

It is known that one of the most important factors, when applying GPR, is the reduction of the ground clutter caused by ground surface roughness and inhomogeneities of the subsurface material. This clutter is spatially random. On the other hand, AP land mine is a relatively large and smooth object compared to other sources of natural clutter, such as gravel and crushed stones. Therefore, the scattered waves from a buried AP land mine are spatially more correlated than from natural objects.

As the clutter masks the response from shallow buried land mines, a special signal processing stage was proposed by Groenenboom et al. [13] to remove the ground surface response and associated clutter components. Average and moving average background subtraction had been used to reduce clutter. Another statistical method of clutter/signal separation based on principal and independent component analysis (PCA/ICA) was introduced by Karlsen et al. [14]. A theoretical study of the clutter reduction algorithm, which used numerically generated rough surface backscattering coefficients, was presented by Salvati et al. [15]. In a surface clutter reduction algorithm, every A-scan signal was modelled as a sum of damped exponentials. A

set of exponentials considered as early time surface clutter was removed further from the GPR data. Expansion of the GPR signal into damped exponentials was employed also in a parametric clutter reduction method by van der Merwe et al.[16]. This method requires precise knowledge about the signal from the buried object. The effects of interaction between the antenna and ground surface were also subtracted using a two-port model representing the radar antenna in [17, 18]. The transfer functions of the two-port were determined using several calibration measurements above a planar metal sheet. Then, the measured signal could be transformed into the reflection coefficient of the electromagnetic wave from the soil and thus all the antenna effects were filtered out. Consequently, the ground surface response could be subtracted as a reflection from the air-soil interface. After suppressing the clutter, the GPR image could be built using migration or synthetic aperture techniques that could enhance the weak target response. However, performance of the synthetic aperture method degraded in case the object is very shallow [19].

In this paper, to avoid both the effect of the ground surface clutter and the antenna coupling in addition of detecting the location of shallow buried objects; a new data analysis technique described in Eqns. (1) and (2) is proposed:

$$\Delta S\left(f\right) = \frac{\left|\left(\mid S_{11,wo}\left(f\right)\mid^2 - \mid S_{11,woo}\left(f\right)\mid^2\right)\right|}{\mid S_{11,woo}\left(f\right)\mid^2} \tag{1}$$

$$\Delta S = \frac{\sum_{f}\left|\left(\mid S_{11,wo}\left(f\right)\mid^2 - \mid S_{11,woo}\left(f\right)\mid^2\right)\right|}{\sum_{f}\mid S_{11,woo}\left(f\right)\mid^2} \tag{2}$$

Where WOO indicates the data measured without object and WO the data with object, f =1, 2…801 is the number of frequency points, S11, wo or woo (f) is received transmission signal at frequency f. The analysis using Eqn. (1) gives the frequency sensitivity indicating the frequencies that are sensitive to the presence of the object, and the indication of the presence of an object. Eqn. (2) gives an overall sensitivity measurement over the frequency range from 9 GHz to 11 GHz. By analyzing the results obtained using Eqn. (2), the location of buried object can be identified, which will be illustrated in Section 2.2.

Experiments Results

According to the scanning dimensions, the GPR data will be presented in three different forms, i.e. A, B and C-Scans. With the definition of the 3D coordinate system shown in Fig. 2 where the X_sOY_s-plane represents the ground surface and the Z_s-axis represents the direction into the ground, the A-scan is a set of measurements at one transmitting and receiving configuration. B-scan is a collection of A-scans along one horizontal direction on the X_sOY_s plane (e.g. X_s-axis), and C-scan is a collection of B-scans along the orthogonal direction on the X_sOY_s plane (e.g. Y_s-axis). In operating the system, firstly A-scan is carried out to present the frequency sensitivity ΔS (f), which is followed by B-scan to calculate overall sensitivity ΔS. Finally, C-scan which will be used to detect the location of shallow buried objects is applied. A, B and C-scans can be considered as 1D, 2D and 3D data respectively [20].

Metallic and plastic objects, with dimensions 6 cm x 6 cm x 3 cm, are used to represent the mine. These objects are placed in a plastic box filled with sand. Fig. 3 shows a metallic object in the sand box with dimensions 30 cm x 30 cm x 30 cm, the metallic object is investigated first. The measurements are made by the VNA, and the data are recorded in the computer. The same procedures are applied to the plastic object.

Metallic object
Figure 3 shows the antennas in the A-scan position, with the metal object buried 2, 6, 10 cm. At this A-scan position, the object is at h = 8, 12, 16 cm from the transmitting antenna respectively (such that antenna height (d) is 6cm as shown in Fig. 1).

The measured transmissions S11 data with and without buried object are analyzed by applying Equation (1). The frequency variations of ΔS (f) due to the presence of the object at h = 12 cm over the frequency range from 9 GHz to 11 GHz are shown in fig. 4. The analysis of the results in Fig. 4 shows that the object's presence can be detected with good sensitivity at a frequency of 10.8 GHz.

Following the first A-scan, a B-scan is carried out to identify the metal object location in the X_s-direction. The B-scan is formed of A-scans with a step distance of 2 cm. The Common Offset (with zero offset) data acquisition technique is applied to collect the data from the first A-scan location, and further 16 A-scan locations. Fig. 5 shows the results of the signal level difference ΔS obtained using Eqn. (2) for different heights h = 12 cm. The location of the buried object can be identified from the B-scan results. The maximum signal level percentage calculated using Eqn. (2) due to the object presence is 8 %.

It can be seen from Fig. 6 that the location of the buried object manually highlighted by a circle can be clarified from the 2D image, which is generated from the proposed data analysis technique. This result needs to be more accurate to obtain the buried object place accurately. This could be done by using bigger sand basket to avoid basket wall clutter, or by working in the real field.

Non-metallic object result
To verify the proposed data analysis technique for non-metallic object detection, the metal object is replaced by a plastic object. The object is buried at a depth of d = 6 cm below surface in a sand box of 30 cm x 35 cm x 32 cm. The antenna height (h) as shown in Fig.1 is maintained at 12 cm.

The analysis of the results in Fig. 7 shows that the plastic object's presence can be detected with good sensitivity at a frequency of 10.9 GHz.

Following the first A-scan, a B-scan is carried out to identify the plastic object location in the X_s-direction. The B-scan is formed of A-scans with a step distance of 2 cm. The Common Offset (with zero offset) data acquisition technique is applied to collect the data from the first A-scan location, and further 16 A-scan locations. Fig. 8 shows the results of the signal level difference ΔS obtained using Eqn. (2) for different heights h = 12 cm. The location of the buried object can be identified from

the B-scan results. The maximum signal level difference percentage calculated using Eqn. (2) due to the object presence is approximately 11 %.

The mine appears in Fig. 8 between steps 8&9 and appear again in step 1&2 and 15&16 which are the plastic edge of the sand bin which seems to be like the electric properties of the plastic mine material.

CONCLUSION

We have proposed a GPR system with one transmitting / receiving antenna and a frequency domain data analysis technique given in Eqns. (1) and (2) which removes the effect of ground surface clutter and minimizes the effect of local ground properties. Furthermore, this technique is found to be not affected by the material type of the buried objects. This system is able to acquire data in the frequency domain from 9 GHz to 11 GHz. By using Common Offset data acquisition, we are able to acquire data in the frequency domain from 9 GHz to 11 GHz.

REFERENCES

[1] Boutros-Ghali, B. "The Land Mine Crisis" Foreign Affairs, Vol. 73, pp 8-13, (1994).

[2] Bourgeois, J. M., and G. S. Smith "complete electromagnetic simulation of the separated-aperture sensor for detecting buried land mines" IEEE Transactions on Antennas and Propagation, Vol. 46, No. 10, pp 1419-1426, (1998).

[3] Nolan R V, Egghart H C, Mittleman L, Brooke R L, Roder F L and Gravitte D L MERADCOM Mine Detection Program 1960–1980 US Army Mobility Equipment Res. Development Command, Fort Belvoir, (1980).

[4] Stewart C Summary of mine detection research US Army Eng. Res. Development Labs, vol 1 and 2, (1960).

[5] Peters, Leon, Jr., Jeffrey J. Daniels, and Jonathan D. Young "Ground penetrating radar as a subsurface environmental sensing tool" Proceedings of the IEEE, Vol. 82, No. 12, pp 1802-1822, (1994).

[6] Sato, M., Fang Guangyou, and Zeng Zhaofa "Landmine detection by a broadband GPR system" Toulouse, France: IEEE, pp 758-760, (2003).

[7] Sato, Motoyuki, Yusuke Hamada, Xuan Feng, Fan-Nian Kong, Zhaofa Zeng, and and Guangyou Fang "GPR Using an Array Antenna for Landmine Detection" Near Surface Geophysics, pp 3-9, (2004).

[8] Brunzell, H. "Clutter reduction and object detection in surface penetrating radar" Edinburgh, UK: IEE, pp 688-691, (1997).

[9] Groenenboom, J., and A. G. Yarovoy "Data processing for a landmine detection dedicated GPR" Goldcoast, Aust: Society of Photo-Optical Instrumentation Engineers, Bellingham, WA, USA, pp 867-871, (2000).

[10] Feng, Xuan, and Motoyuki Sato "Pre-stack migration applied to GPR for landmine detection" Inverse Problems, Vol. 20, No. 6, pp 99-115, (2004).

[11] Sato, M., and X. Feng "GPR migration algorithm for landmines buried in inhomogeneous soil" Washington, DC, USA: IEEE, pp 206-209, (2005).

[12] Yarovoy, A., P. Aubry, P. Lys, and L. Ligthart "UWB array-based radar for landmine detection." Manchester, UK: IEEE, pp 186-189, (2006).

[13] Groenenboom, J., and and A. Yarovoy "Data processing and imaging in GPR system dedicated for landmine detection" Subsurf. Sens. Technol. Appl., Vol. 3, pp 387– 402, (2002).

[14] Karlsen, Brian, Jan Larsen, Helge B. D. Sorensen, and Kaj B. Jakobsen "Comparison of PCA and ICA based clutter reduction in GPR systems for anti-personal landmine detection" pp 146-149, (2001).

[15] Salvati, J. L., C. C. Chen, and J. T. Johnson "Theoretical study of a surface clutter reduction algorithm" Vol. 3, pp 1460-1462, (1998).

[16] van der Merwe, A., and I. J. Gupta "A novel signal processing technique for clutter reduction in GPR measurements of small, shallow land mines," IEEE Transactions on Geoscience and Remote Sensing, Vol. 38, No. 6, pp 2627-2637, (2000).

[17] Lopera, O., E. C. Slob, N. Milisavljevic, and S. Lambot "Filtering soil surface and antenna effects from GPR data to enhance landmine detection" IEEE Transactions on Geoscience and Remote Sensing, Vol. 45, No. 3, pp 707-717, (2007).

[18] Mikhnev, V. A., and P. Vainikainen "Single-reference near-field calibration procedure for step-frequency ground penetrating radar" IEEE Transactions on Geoscience and Remote Sensing, Vol. 41, No. 1, pp 75-80, (2003).

[19] Potin, D., E. Duflos, and P. Vanheeghe "Landmines ground-penetrating Radar signal enhancement by digital filtering" IEEE Transactions on Geoscience and Remote Sensing, Vol. 44, No. 9, pp 2393-2406, (2006).

[20] Jing, Zhang, and B. Nath "Processing and analysis of ground penetrating radar landmine detection" Ottawa, Ont., Canada: Springer-Verlag, pp 1204-1209, (2004).
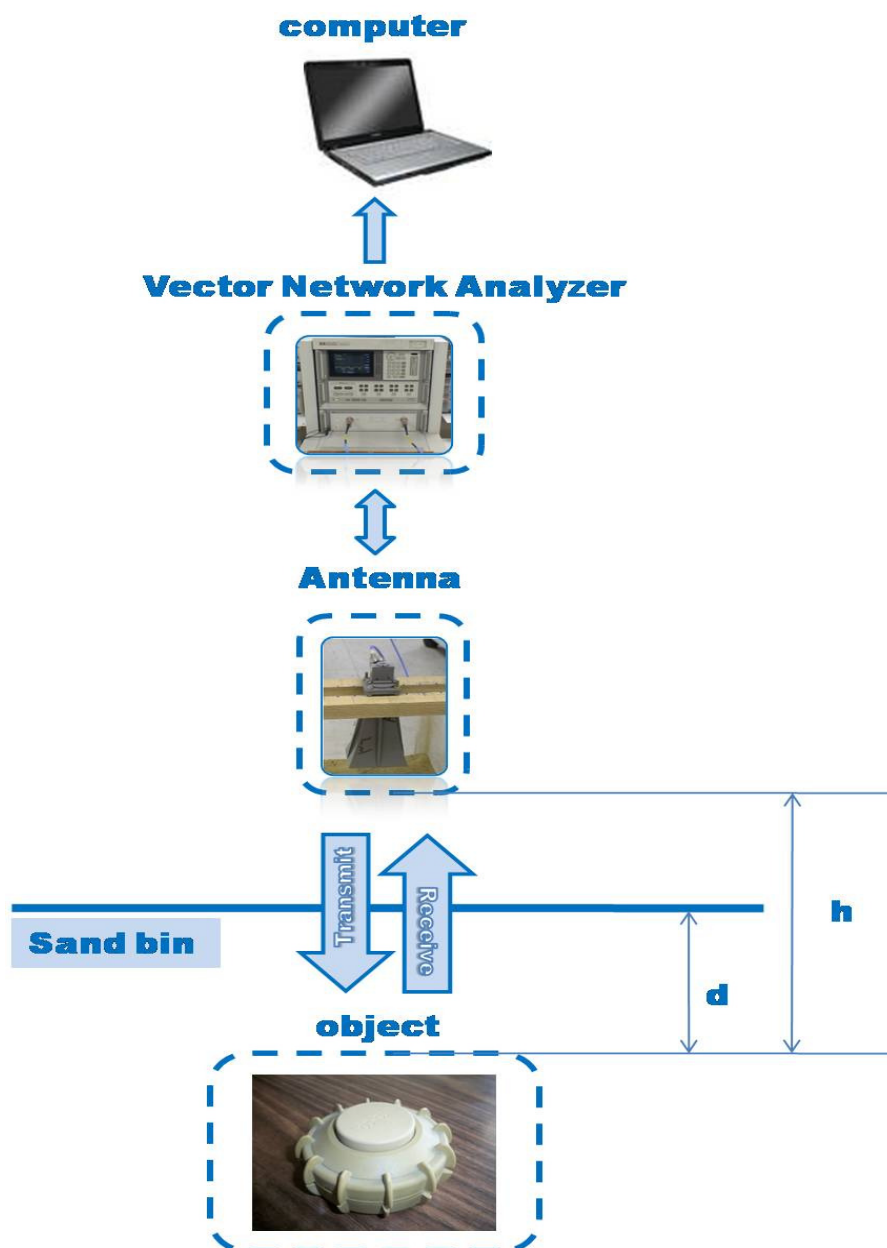
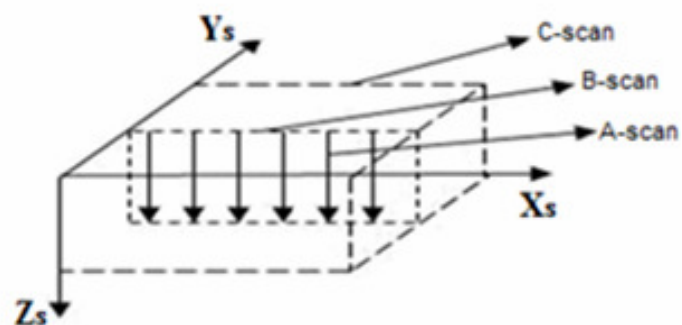**Fig. 1.** Block diagram of the proposed GPR system and WARR data acquisition.

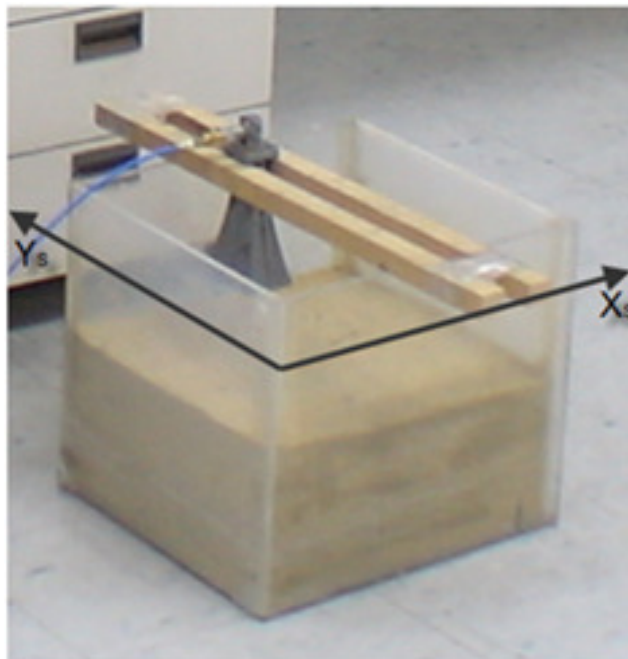**Fig. 2.** 3D coordinate system defined on the ground section.

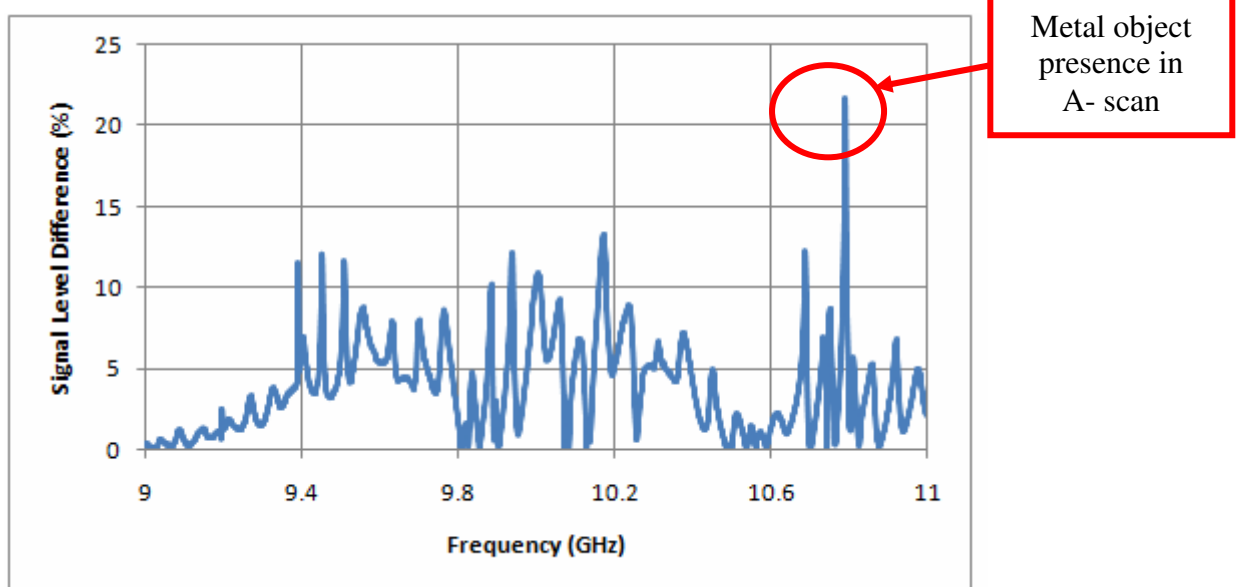**Fig. 3.** Antenna in a position on the metal object .

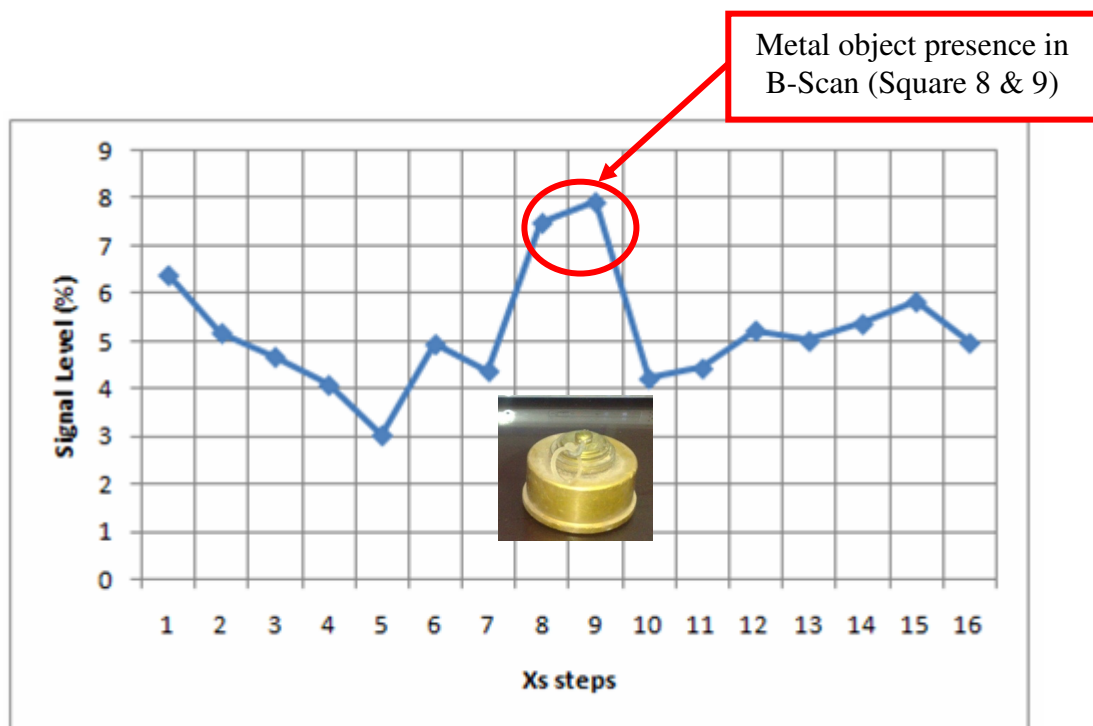**Fig. 4.** Frequency response of the antenna due to the presence of the metallic buried object (A-scan).

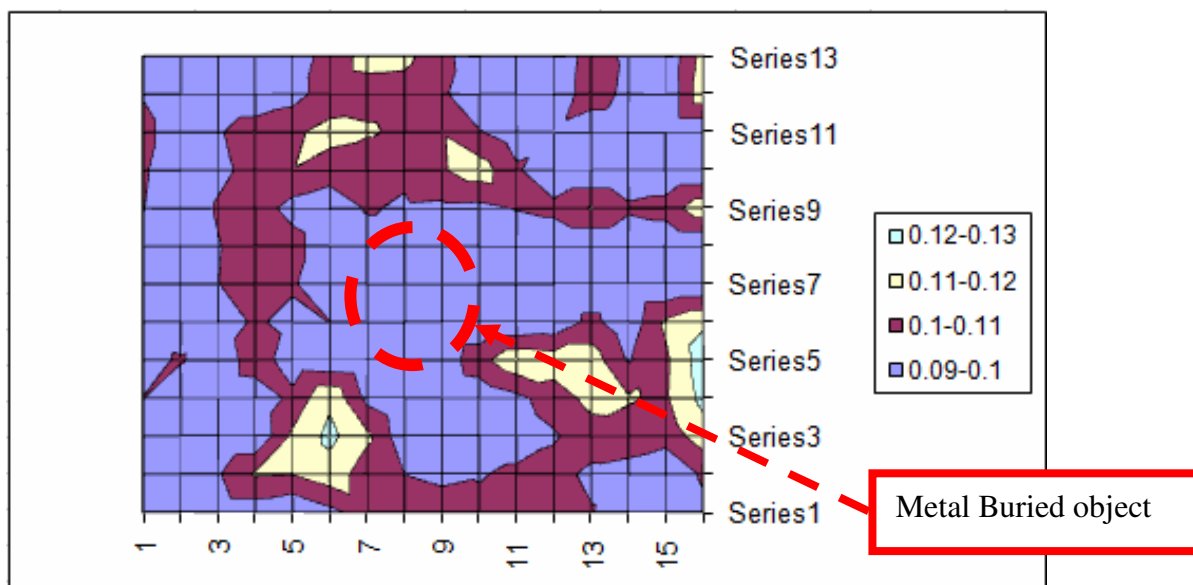**Fig. 5.** Signal level difference Vs antenna position for metallic object location (B-scan).

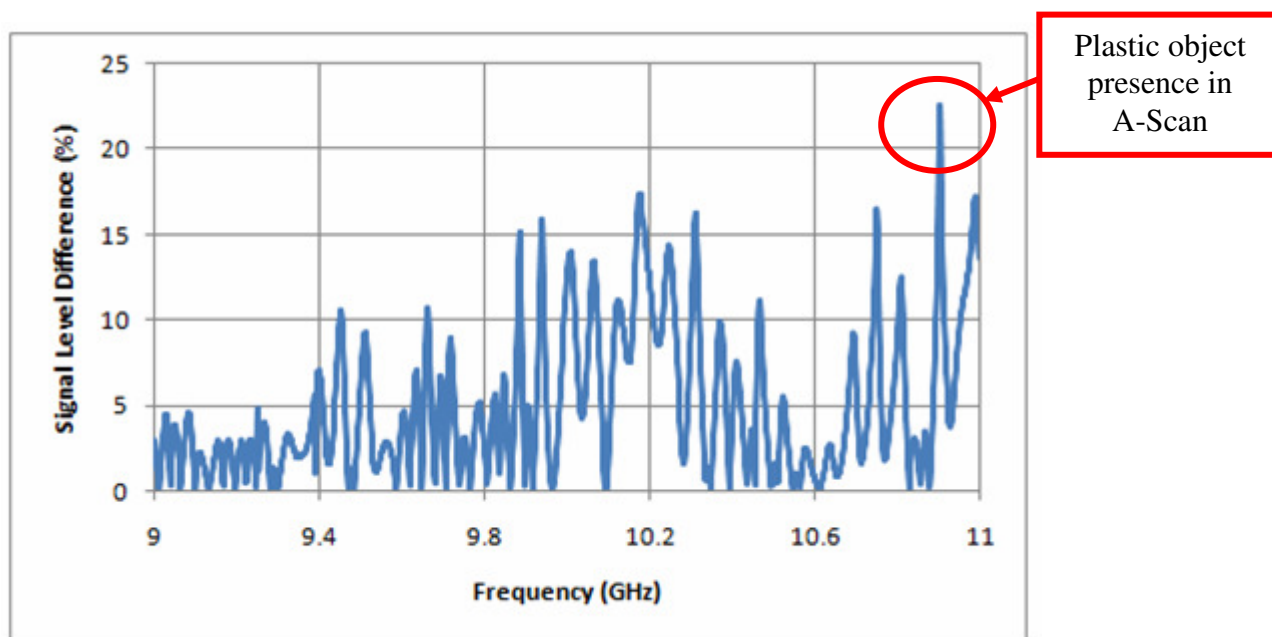**Fig. 6.** 2D image of metal objects buried in dry sand.

Fig. 7. Frequency response of the antenna due to the presence of the plastic buried object (A-scan).
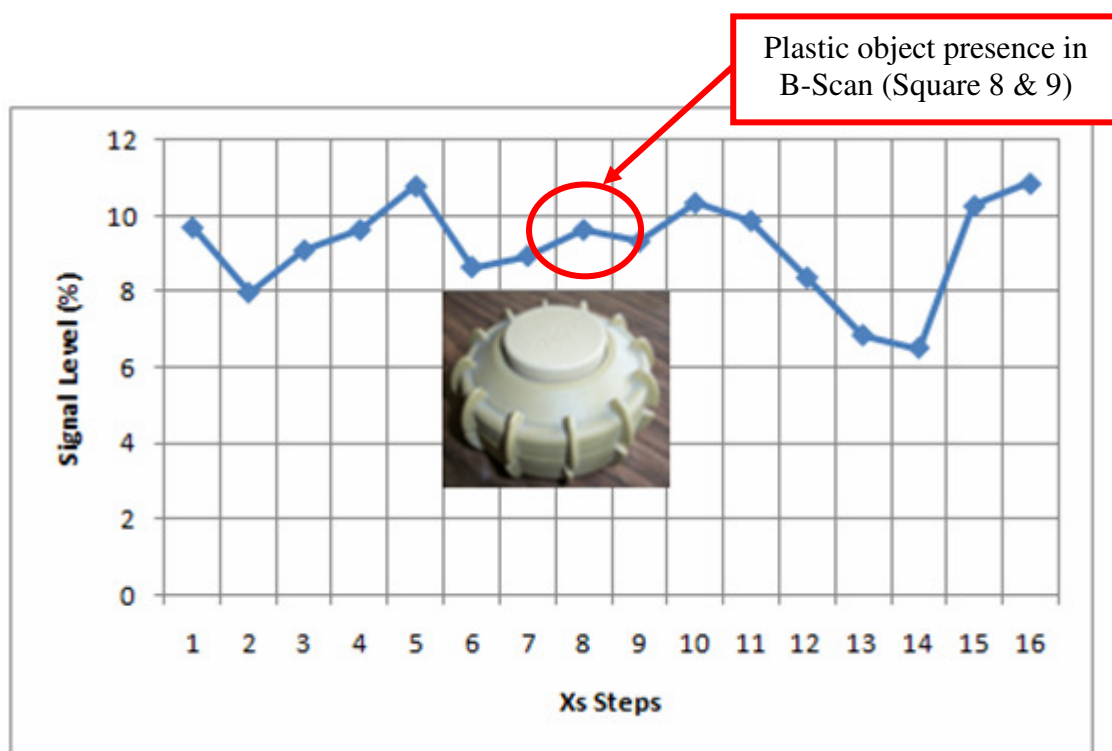

Fig. 8. Signal level difference vs antenna position for plastic object location (B-scan) illustrating presence of bin borders.